J Fluoresc (2013) 23:1229–1237
DOI 10.1007/s10895-013-1254-2

ORIGINAL PAPER

Fluorescence Study of the Membrane Effects of Aggregated Lysozyme

Olga K. Kutsenko · Valeriya M. Trusova · Galyna P. Gorbenko · Anna S. Lipovaya · Ekaterina I. Slobozhanina · Lyudmila M. Lukyanenko · Todor Deligeorgiev · Aleksey Vasilev

Received: 22 April 2013 / Accepted: 17 June 2013 / Published online: 28 June 2013

Abstract The last decade has seen unprecedented upsurge of interest in the structural and toxic properties of particular type of protein aggregates, amyloid fibrils, associated with a number of pathological states. In the present study fluorescence spectroscopy technique has been employed to gain further insight into the membrane-related mechanisms of amyloid toxicity. To this end, erythrocyte model system composed of liposomes and hemoglobin was subjected to the action of oligomeric and fibrillar lysozyme. Acrylamide quenching of lysozyme fluorescence showed that solvent accessibility of Trp_{62} and Trp_{108} increases upon the protein fibrillization. Resonance energy transfer measurements suggested the possibility of direct complexation between hemoglobin and aggregated lysozyme. Using the novel squaraine dye SQ-1 it was demonstrated that aggregated lysozyme is capable of inhibiting lipid peroxidation processes. Fluorescent probes pyrene, Prodan and diphenylhexatriene were employed to characterize the membrane-modifying properties of hemoglobin and lysozyme. Both oligomeric and fibrillar forms of lysozyme were found to exert condensing influence on lipid bilayer structure, with the membrane effects of fibrils being less amenable to modulation by hemoglobin.

O. K. Kutsenko · V. M. Trusova · G. P. Gorbenko · A. S. Lipovaya
Department of Nuclear and Medical Physics, V.N. Karazin Kharkiv National University, 4 Svobody Sq, Kharkiv 61022, Ukraine

E. I. Slobozhanina · L. M. Lukyanenko
Laboratory of Medical biophysics, Institute of Biophysics and Cell Engineering, National Academy of Sciences of Belarus, Academicheskaya str., 27, Minsk 220072, Belarus

T. Deligeorgiev · A. Vasilev
Department of Applied Organic Chemistry, Faculty of Chemistry, University of Sofia, 1164 Sofia, Bulgaria

V. M. Trusova (✉)
19-32 Geroyev Truda Str, Kharkov 61144, Ukraine
e-mail: valtrusova@yahoo.com

Keywords Hemoglobin · Liposomes · Aggregated lysozyme · Lipid peroxidation · Fluorescence spectroscopy

Introduction

During the past decades the phenomenon of protein self-assembly into highly ordered supramolecular aggregates called amyloid fibrils attracts ever growing attention due to a well established correlation between the deposition of these aggregates in various tissues and etiology of numerous severe disorders including Alzheimer's, Creutzfeldt-Jacob's, Parkinson's, Huntington's diseases, systemic amyloidosis, type II diabetes, etc. [1]. Increasing evidence indicates that interactions between amyloid fibrils and cell plasma membranes may essentially contribute to amyloid cytotoxicity [2–4]. Red blood cells are known to be one of the targets for pathological fibrillar aggregates. Specifically, amyloid-β peptide was reported to induce eryptosis [5] and affect metabolic modulation of red blood cells [6–8]. The increased erythrocyte membrane fluidity was found in Alzheimer disease [9, 10]. The binding of amyloid proteins to erythrocyte membranes is followed by the oxidative stress of red blood cells [8, 11]. Furthermore, fibrillar proteins can exert influence on erythrocyte functioning through their association with hemoglobin [12]. However, despite extensive research efforts, molecular details of amyloid-induced erythrocyte damage are far from being fully understood. To approach this problem, in the present study we employed fluorescence spectroscopy technique to ascertain the effects of lysozyme oligomers and mature fibrils on the liposomal erythrocyte model system.

Erythrocyte model system composed of unilamellar lipid vesicles and hemoglobin (Hb) was chosen for the following reasons. It was found that hemoglobin possesses the ability to associate with the inner membrane of red blood cells [13, 14]. Erythrocyte membrane has two types of Hb binding

sites. The sites of first type, that include band 3 protein, are characterized by high affinity, reversibility and anticooperativity of binding [15, 16]. When bound to band 3 protein Hb resides on the membrane surface and do not insert into the lipid bilayer. The low-affinity Hb binding sites of second type consist of phospholipids [17]. Although Hb-lipid interactions have long been a focus of numerous studies, precise molecular mechanisms as well as physiological implications of Hb-lipid binding still remain unclear. Adsorption of proteins onto lipid bilayers is a multistep process including interdependent protein conformational changes and membrane structural modifications. Hb-lipid binding is driven by both electrostatic and hydrophobic interactions [18, 19]. Non-polar coupling promotes protein penetration into the inner membrane regions that is accompanied by the protein and bilayer structural changes [20, 21] and free-radical production [22, 23].

Experimental

Materials

Egg white lysozyme (Lz), hemoglobin from bovine blood in met form (Hb), acrylamide, 1,3,5-hexatriene (DPH), 6-propionyl-2-dimethylaminonaphthalene (Prodan) and pyrene were from Sigma (USA). Egg yolk phosphatidylcholine (PC) and beef heart cardiolipin (CL) were purchased from Biolek (Kharkov, Ukraine). Cholesterol (Chol) was from Avanti Polar Lipids Inc., (Alabaster, AL). Phospholipids gave single spot by thin layer chromatography in the solvent system chloroform:methanol:acetic acid:water, 25:15:4:2, v/v. SQ-1 was synthesized as described previously [24]. All other chemicals were of analytical grade.

Preparation of Lipid Vesicles

Unilamellar lipid vesicles composed of PC and its mixtures with 5 mol% CL (CL5) and 10 mol% CL (CL10) or 30 mol% Chol (Chol30) were prepared using the extrusion technique [25]. Appropriate amounts of lipid ethanol solutions were evaporated to dryness under vacuum to remove organic solvent. The obtained lipid films were subsequently hydrated with 1.2 ml of 5 mM Na-phosphate buffer (pH 7.4). The resulting dispersions were extruded through a 100 nm pore size polycarbonate filter (Nucleopore, Pleasanton, CA). The lipid concentration determined according to the procedure of Bartlett [26] was 10 mM.

Formation of Amyloid Fibrils

The reaction of lysozyme fibrillization was initiated using the approach developed by Holley et al. [27]. Protein solutions (3 mg/ml) were prepared by dissolving lysozyme in deionized water with subsequent slow addition of ethanol to a final concentration 80 %. Next, the samples were subjected to constant agitation at ambient temperature. This resulted in the formation of lysozyme fibrils over a time course of about 30 days. The amyloid nature of fibrillar aggregates was confirmed in ABM and ANS fluorescence assays. For fluorescent measurements with pre-fibrillar lysozyme aggregates the aliquots of agitated protein solution were taken during the lag-phase (within 10 days of fibrillization).

Fluorescence Measurements

All fluorescence measurements were performed in 5 mM sodium phosphate buffer, pH 7.4, at room temperature. Fluorescence spectra were recorded with Perkin Elmer LS55 (UK) spectrofluorimeter. Excitation wavelengths were 340 nm for pyrene, 350 nm for DPH and Prodan, 640 nm for SQ-1. SQ-1 fluorescence kinetic measurements were monitored at 676 nm. Excitation and emission slit widths were set at 2.5 nm for pyrene, 5 nm for Prodan, 10 nm for SQ-1 and 15 nm for DPH.

Fluorescence quenching data were analyzed using the Stern-Volmer equation:

$$\frac{I_0}{I} = 1 + k_q\tau_0 = 1 + K_{SV}[Q] \tag{1}$$

where I_0 and I are fluorescence intensities of Lz in the absence and presence of a quencher, k_q—bimolecular quenching constant, τ_0 is fluorophore lifetime in the absence of quencher, K_{SV}—Stern-Volmer constant, $[Q]$—quencher concentration.

Prodan three-wavelength generalized polarization (*3wGP*) was calculated according to the following relationships [28]:

$$3wGP = \frac{R_{12}-1}{R_{12}+1};\ R_{12} = \frac{I_1 k_{32}}{I_2 k_{32} - I_3 + I_1 R_{31}};\ k_{32} = I_{3W}\Big/I_{2W};\ R_{31} = I_{3M}\Big/I_{1M} \tag{2}$$

where I_1, I_2, I_3 are fluorescence intensities of Prodan at 420, 480 and 530 nm, respectively; I_{2W}, I_{3W}, I_{1M}, I_{3M} are fluorescence intensities of Prodan in water (subscript *W*) and membrane (subscript *M*) at 420 and 530 nm, respectively.

For quantitative analysis of resonance energy transfer between Trp residues of Lz and heme group of Hb the measured fluorescence intensities of the donor were corrected for the inner filter and reabsorption effects using the following coefficient:

$$k = 10^{(A_{ex}+A_{em})/2} \tag{3}$$

where A_{ex} and A_{em} are the acceptor optical densities at the excitation and emission wavelengths, respectively. The

Förster radius (R_0) for Trp-heme donor-acceptor pair was calculated as:

$$R_0 = 979\left(\kappa^2 n_r^{-4} Q_D J\right)^{1/6}, J = \int_0^\infty F_D(\lambda)\varepsilon_A(\lambda)\lambda^4 d\lambda \Big/ \int_0^\infty F_D(\lambda)d\lambda \quad (4)$$

where J is the overlap integral derived from numerical integration, $F_D(\lambda)$ is the donor fluorescence intensity, ε_A (λ) is the acceptor molar absorbance at the wavelength λ, n_r is the refractive index of the medium (n_r=1.37), Q_D is the donor quantum yield, κ^2 is the orientation factor. Forster radius for Trp-heme donor-acceptor pair was found to be~3.9 nm. The average distance R between Trp and heme moieties was determined from [29]:

$$E = \frac{R_0^6}{R_0^6 + R^6} \quad (5)$$

where E is the efficiency of energy transfer, E=1−I/I_0, I, I_0 are the donor fluorescence intensities in the absence and presence of acceptor, respectively.

Results and Discussion

Quenching of Lysozyme Fluorescence by Acrylamide

To elucidate the nature of lysozyme conformational changes upon fibrillization, at the first step of the study we examined the quenching of Lz intrinsic fluorescence by acrylamide. Lz contains 6 Trp residues, of which Trp_{28} and Trp_{111} are located in the hydrophobic core, while Trp_{62}, Trp_{63}, Trp_{108} and Trp_{123} reside on the surface of protein molecule [30, 31]. Two of these residues, Trp_{62} and Trp_{108} are known to be the predominant Lz fluorophores, responsible for ~80 % of the total protein emission [30]. Therefore, the measured quenching efficiency mainly reflects solvent accessibility of these two Trp residues. As seen in Table 1, within the first 10 days of protein incubation, corresponding to the lag phase of fibrillization process, the differences between Stern-Volmer constants were insignificant, while for the mature fibrils abundant on the 30-th day of fibrillization K_{SV} value exhibited a marked increase. Several lines of evidence clearly indicate that lysozyme amyloid formation proceeds via partially unfolded conformational states [32]. As was demonstrated by Holley and coauthors, in 80 % ethanol Lz adopts a relatively stable structure similar to that in the native state [27]. However, ethanol in combination with agitation turned out to induce pronounced partial unfolding of lysozyme, which occurs during the lag phase. In predominantly organic solvents hydrophobic interactions between side chains become weaker, thereby promoting the exposure of non-polar protein core [33]. Dynamic light-scattering studies showed that in 80 % ethanol lysozyme tend to adopt flexible "broken rod" conformation favorable for the formation of intermolecular β-sheets [34]. Hence, the fluorescence quenching data presented here can be interpreted in terms of the differences between Lz conformations in the lag phase and at the end of fibrillization process. As judged from CD measurements, the β-sheet content of Lz increases during the lag phase, presumably due to formation of dimers from the partially unfolded protein monomers [27]. It seems likely that in the course of fibril growth monomeric subunits undergo further structural reorganization resulting in the increased solvent accessibility of Trp_{62} and Trp_{108}.

Table 1 Stern-Volmer constants for quenching of lysozyme tryptophan fluorescence by acrylamide

Time of lysozyme incubation under denaturing conditions, days	K_{SV}, M^{-1}
2	3.35±0.08
4	3.00±0.15
6	4.19±0.09
8	4.00±0.04
10	3.34±0.10
30 (amyloid fibrils)	6.08±0.07

Lysozyme Association with Hemoglobin

At the second step of the study it was of interest to evaluate whether Lz oligomers and fibrils can directly associate with other proteins. To this end, the resonance energy transfer (RET) technique was employed for monitoring the interaction between Lz and Hb being employed as a model protein. Trp residues of Lz served as the energy donors, while heme groups of Hb were employed as the acceptors. As illustrated in Fig. 1, Hb

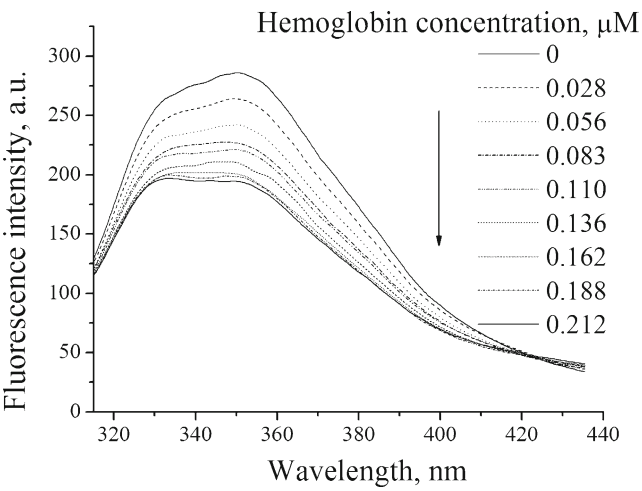

Fig. 1 Decrease of amyloid lysozyme tryptophan fluorescence in the presence of hemoglobin. Lysozyme concentration was 1 μM

addition to oligomeric or fibrillar Lz was followed by the quenching of Trp fluorescence without any shift of emission maximum. Lysozyme emission spectra were corrected for the inner filter effects (Eq. (3)) to ensure that the quenching Lz fluorescence arises from RET, rather than from the absorption of exciting and emitted light by the heme groups. It appeared that the efficiency of energy transfer between Lz and Hb is virtually independent of the time of Lz incubation under denaturing conditions. The average donor-acceptor distance calculated from the Eq. (5) was found to be~4.4 nm. Within Hb concentration range employed in the RET experiments (0–0.2 μM), Hb tetramer tends to dissociate into αβ dimers [35]. Given that dimensions of Hb dimer are approximately 4.2×4.0×5.0 nm, while the size of Lz molecule is about 4.5×3.0×3.0 nm, the above estimate for Trp-heme separation seems to be quite reasonable. Since at physiological pH Lz bears high positive charge, while Hb is practically uncharged, it is hardly probable that electrostatic interactions play determining role in Lz-Hb association. Presumably, the formation of intermolecular Lz-Hb contacts is driven mainly by hydrophobic interactions between the exposed non-polar patches. Fibrillization may give rise to the increase of protein surface hydrophobicity, as was demonstrated, for instance, for Aβ-peptide [36]. The exposure of non-polar amino acid residues upon Lz incubation of in 80 % ethanol and Hb dissociation into dimers [37] may be important determinants of the observed Lz-Hb complexation.

Lysozyme Influence on Hemoglobin-Induced Lipid Peroxidation

One of the known mechanisms of amyloid-mediated erythrocyte damage involves induction of oxidative stress [8, 11]. Free radical reactions in a lipid phase can also be initiated by hemoglobin-membrane interactions [38–40]. Therefore, a separate series of our experiments was designed to ascertain whether oligomeric and fibrillar forms of Lz can modulate the process of lipid peroxidation. For this purpose, we used the fluorescence-based approach exploiting high sensitivity of the novel squaraine dye SQ-1 to the presence of free radicals. It has been previously found that Hb-induced lipid peroxidation brings about drastic quenching of SQ-1 fluorescence, presumably arising from the cleavage of dye squaric moiety by the reactive oxygen species [41]. In the present study we employed SQ-1 to monitor oxidative processes in the model systems containing liposomes, Hb and Lz. SQ-1 incorporated into liposomal membranes appeared to be insensitive to Lz-induced membrane modifications, while Hb produced significant decrease in SQ-1 fluorescence. Oligomeric or fibrillar Lz was added to liposomes pre-incubated with SQ-1 and kinetics of the probe fluorescence was monitored at SQ-1 emission maximum (676 nm) over 3–5 min. Then Hb was added to the system and kinetic measurements were performed over 6–10 min. As illustrated in Fig. 2, SQ-1 fluorescence quenching was considerably suppressed in the presence of lysozyme. Interestingly, the magnitude of this effect was practically independent of the protein aggregation state varying with increasing the time of its incubation under denaturing conditions. There are at least two possible explanations for these findings. First, Lz can be a scavenger of free radicals. Positively charged Lz molecule initially associates with the lipid bilayer surface via formation of ionic contacts between the charged amino acid residues and lipid headgroups. Then, initial electrostatic binding is followed by the protein partial insertion into a membrane

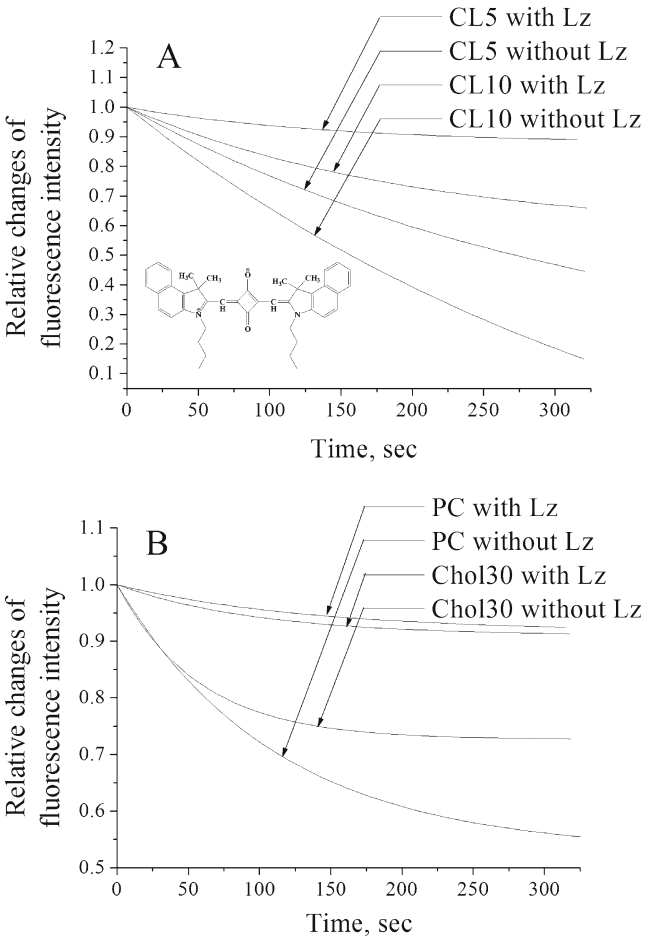

Fig. 2 Relative changes of fluorescence intensity of SQ-1 upon hemoglobin binding to CL5, CL10 (**a**) and PC, Chol30 (**b**) lipid vesicles in the presence and absence of amyloid lysozyme. Lipid concentration was 15.5 μM, lysozyme −2 μM, SQ-1 −0.12 μM, hemoglobin −0.02 μM. Shown in inset is chemical structure of SQ-1

hydrophobic core. Presumably, some molecular groups of lysozyme (for instance, SH-groups) can react with free radicals, thereby preventing the initiation and propagation of oxidative chain reaction. Since Lz has higher affinity for anionic lipids, in CL-containing bilayers its antioxidant effect was more pronounced compared to the neat PC membranes, as shown in Fig. 2. According to the second hypothesis, Lz antioxidant effect may originate from the competition between Hb and Lz for the membrane binding sites. In addition, as was demonstrated above, Lz avidly associates with Hb, therefore, aggregated protein can serve as a template for Hb binding. All the above types of protein-lipid and protein-protein interactions may hamper Hb ability to induce lipid peroxidation.

Hemoglobin Effect on Lipid Bilayer Structure

At the next step of the study we examined the influence of hemoglobin on membranotropic activity of lysozyme. First, Hb ability to modify lipid bilayer structure was assessed using several fluorescent probes differing in their bilayer location. Structural changes induced by Hb in the headgroup membrane region were monitored with polarity-sensitive probes pyrene and Prodan. Pyrene monomers are known to reside in the acyl chain region close to the lipid headgroups [42]. Relative intensity of the first-to-third pyrene vibronic peaks (I_I/I_{III}) is highly sensitive to microenvironmental polarity [43, 44]. This parameter was~1 for all types of liposomes, showing no explicit dependence on lipid composition of the model membranes. Hb-lipid interactions resulted in the rise of I_I/I_{III} value by ~12–18 %, indicating an increase in the lipid bilayer polarity. These findings are in agreement with the data previously reported by Xi et al. [45]. Presumably, Hb-lipid binding destabilizes headgroup region of the lipid bilayer, thereby promoting water penetration into the membrane interior. Additional arguments in favour of this assumption were obtained using another polarity-sensitive probe, Prodan. This probe displays bimodal membrane distribution, which depends on the packing properties of a lipid bilayer. The ratio of fluorescence signals originating from Prodan molecules occupying different membrane sites is highly sensitive to the probe environmental polarity [46]. As shown in Fig. 3, Hb-lipid binding resulted in the decrease of *3wGP* value, being indicative of the increase in membrane polarity [28]. Higher magnitudes of *3wGP* changes produced by Hb in CL-containing liposomes compared to PC can be explained by the fact that electrostatic interactions between Hb and lipid headgroups destabilize protein structure, giving rise to the formation of partially unfolded state which favors protein incorporation into the membrane core [20, 21]. Drastic decrease of *3wGP* value in Chol30 liposomes could be the result of Hb-induced displacement of Prodan molecules into more polar membrane binding sites.

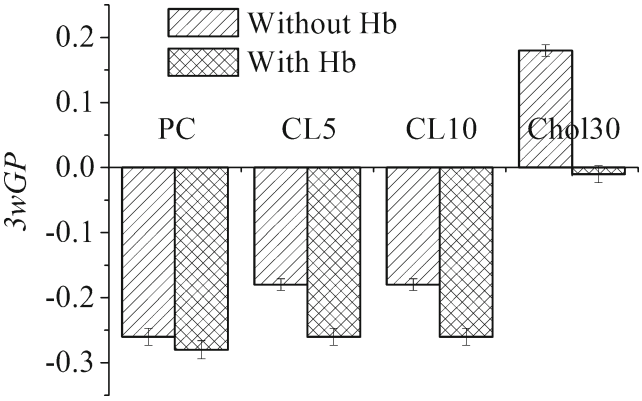

Fig. 3 Three-wavelength generalized polarization of Prodan in lipid and hemoglobin-lipid systems. Lipid, hemoglobin and Prodan concentrations were 38.6 μM, 0.05 μM and 0.3 μM, respectively

Next, using nonpolar fluorescent probes DPH and pyrene we addressed the question of whether Hb can exert influence on the structural state of hydrophobic membrane region. As seen in Fig. 4, Hb interaction with PC and PC/CL liposomes was followed by the increase of DPH anisotropy, resulting from restriction of the probe rotational mobility. These data are consistent with the observation that Hb is capable of increasing membrane viscosity [47]. On the contrary, in Chol30 lipid bilayers DPH anisotropy did not undergo any statistically significant change, suggesting that tighter lateral packing of hydrocarbon chains caused by cholesterol hampers Hb penetration into the membrane interior. Further support for these assumptions comes

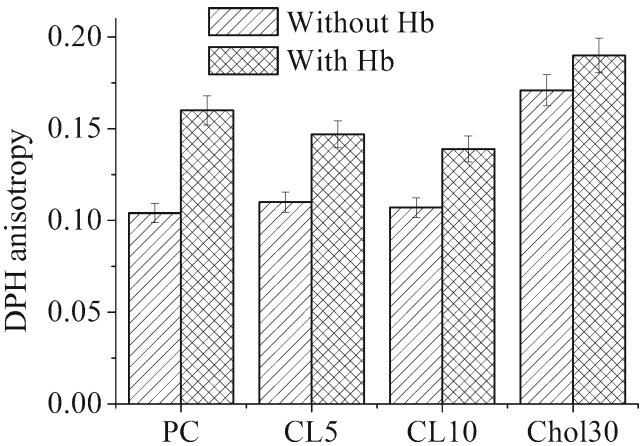

Fig. 4 DPH fluorescence anisotropy in lipid and hemoglobin-lipid systems. Lipid, hemoglobin and DPH concentrations were 38.6 μM, 0.05 μM and 0.9 μM, respectively

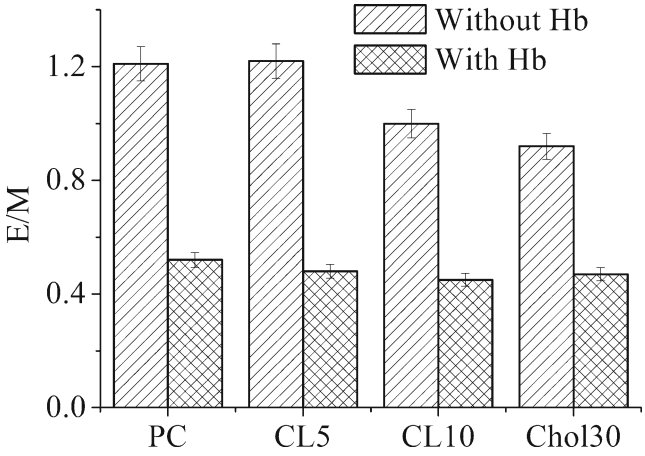

Fig. 5 Pyrene excimer-to-monomer fluorescence intensity ratio in lipid and hemoglobin-lipid systems. Lipid, hemoglobin and pyrene concentrations were 15.7 μM, 0.02 μM and 0.4 μM, respectively

from pyrene excimerization studies. As seen in Fig. 5, Hb-lipid interaction was accompanied by the decrease of excimer-to-monomer intensity ratio (E/M). The amount of excimers (excited-state dimers formed from excited and non-excited pyrene monomers) is determined by the rate of the probe lateral diffusion, which, in turn, is a function of the membrane fluidity, or, more strictly speaking, free volume of a lipid bilayer [48, 49]. The observed decrease in the extent of pyrene excimerization most likely reflects reduction of the bilayer free volume upon Hb penetration into acyl chain membrane region.

Modulation of Lysozyme-Induced Changes in Membrane Structure by Hemoglobin

Further series of experiments was aimed at examining the influence of aggregated lysozyme on structural organization of the model membranes. Likewise, it was of interest to ascertain whether membrane-modifying properties of Lz can be modulated by hemoglobin. The binding of oligomeric and fibrillar Lz to liposomal membranes had no influence on the intensity ratio of the first-to-third pyrene vibronic peaks, indicating that degree of bilayer hydration remained virtually unchanged at the level of upper acyl chain carbons, where pyrene monomers tend to reside. In the meantime, another parameter derived from pyrene emission spectra, excimerization degree, exhibited pronounced decrease upon association of aggregated lysozyme with liposomes (Fig. 6). The magnitude of this effect showed a general trend to increase with the time of Lz incubation under denaturing conditions. Likewise, the age of Lz aggregates turned out to be essential in determining the character of Hb modulating effect on the membrane modifications produced by Lz. As

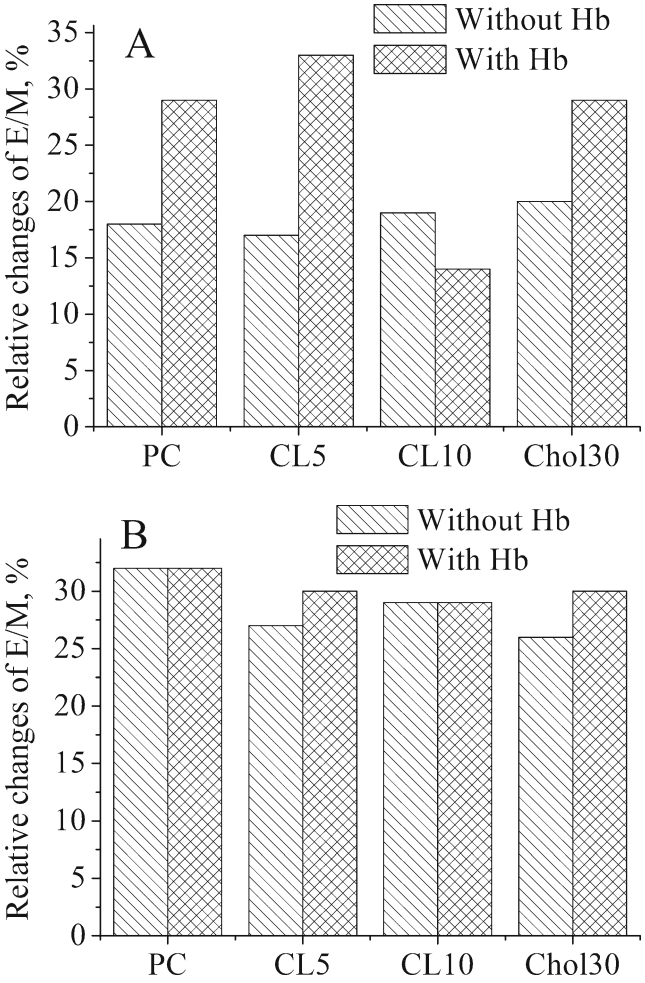

Fig. 6 Relative decrease of pyrene excimer-to-monomer fluorescence intensity ratio upon binding of the lysozyme oligomers (**a**) and fibrils (**b**) to lipid and hemoglobin-lipid membranes. Lipid, hemoglobin, lysozyme and pyrene concentrations were 15.7 μM, 0.02 μM, 2.9 μM and 0.4 μM, respectively

illustrated in Fig. 6, during the lag phase the sign and magnitude of Hb modulating effect on E/M value markedly vary, while E/M changes induced by the mature Lz fibrils were virtually unaffected by Hb. These data reflect the complexity of fibril formation process, with a diversity of membrane-active protein species co-existing during the lag phase. On the contrary, at the end of fibrillization the mature Lz fibrils become predominant components of the examined system and membrane effects of pre-fibrillar species seem to be negligible. Our pyrene excimerization studies indicate that lysozyme is capable of reducing the bilayer free volume in both oligomeric and fibrillar forms, but membrane condensation caused by fibrils is more profound and less subjected to various impacts, as can be deduced from the experiments with Hb. Additional support for these rationales comes from

DPH anisotropy measurements. As shown in Fig. 7, DPH anisotropy changes were markedly modulated by Hb only in the case of Lz oligomers, rather than mature fibrils. Similar to pyrene, DPH responses to mature fibrils were more pronounced compared to oligomers. However, in contrast to pyrene, the effects observed with DPH showed clear dependence on liposome composition. In the negatively charged PC/CL bilayers DPH anisotropy increases under the influence of both oligomeric and fibrillar Lz, suggesting the restriction of the probe rotational mobility. The enhancement of this effect with the rise in CL proportion points to essential role of electrostatics in the membrane structural modifications induced by Lz. Electrostatic interactions ensure protein targeting to the membrane surface, its accumulation at lipid-water interface, specific orienting and structural transformation of polypeptide chain. Obviously, the extent of Lz penetration into membrane core depends on the surface coverage, which, in turn, is governed by electrostatics. The validity of this viewpoint is confirmed by the findings

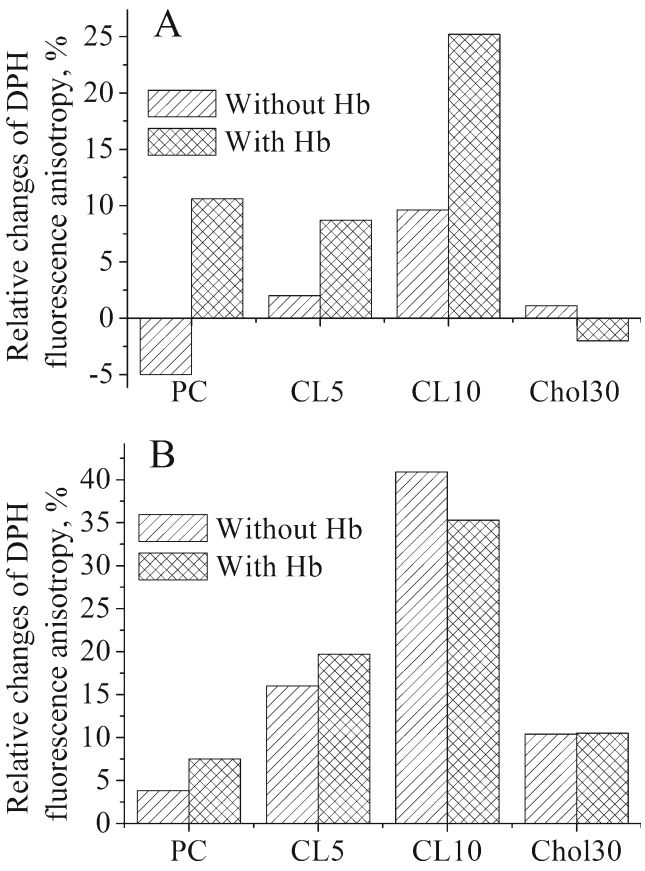

Fig. 7 Relative changes of DPH fluorescence anisotropy upon the binding of lysozyme oligomers (**a**) and fibrils (**b**) to lipid and hemoglobin-lipid membranes. Lipid, hemoglobin, lysozyme and DPH concentrations were 38.6 μM, 0.05 μM, 2.9 μM and 0.9 μM, respectively

that in neutral PC and PC/Chol liposomes DPH anisotropy changes are much smaller than those in PC/CL liposomes (Fig. 7). Moreover, tighter acyl chain packing in Chol-containing bilayer resulted in the absence of any significant anisotropy changes in the case of Lz oligomers and rather small (~5 %) increase of this parameter in the case of Lz fibrils. At last, the distinctions between spectral responses of pyrene and DPH are likely to originate from the differences in the underlying molecular events and bilayer perturbation scales. While the rate of DPH rotational diffusion is sensitive to bilayer perturbation in the immediate vicinity of the probe, the rate of pyrene lateral diffusion determining the excimerization degree is a more integral parameter averaged over entire bilayer volume. The modulating effect of Hb on the bilayer-modifying properties of Lz can be rationalized as follows. The recovered destabilization of the headgroup bilayer region upon Hb-lipid binding can increase the accessibility of the bilayer interior to Lz oligomers, so that the membrane effects detected with pyrene and DPH become more pronounced in the presence of Hb (Figs. 6a and 7a). In contrast, mature fibrils seem to overcome the energetic barrier for membrane insertion more easily compared to oligomers, in a way that does not require bilayer destabilization.

In summary, the results presented here allowed us to suggest the following ideas: (i) in the course of fibril growth monomeric subunits of lysozyme experience structural transformation resulting in the increased solvent accessibility of Trp_{62} and Trp_{108}; (ii) surface hydrophobicity of lysozyme increases upon fibrillization, thereby elevating the likelihood of protein-protein complexation; (iii) regardless of its aggregation state, lysozyme can inhibit the process of lipid peroxidation; (iv) both oligomeric and fibrillar forms of lysozyme can induce condensation of lipid bilayer; (v) membrane-modifying properties of oligomeric lysozyme can be modulated by other proteins. Although these ideas require further experimental verification, they can be regarded as a starting point on the way to deeper understanding of the membrane-mediated mechanisms of amyloid toxicity.

Acknowledgments The work was supported by the grant from the Fundamental Research State Fund (project number F54.4/015).

References

1. Stefani M (2004) Protein misfolding and aggregation: new examples in medicine and biology of the dark side of the protein world. Biochim Biophys Acta 1739:5–25

2. Butterfield SM, Lashuel HA (2010) Amyloidogenic protein-membrane interactions: mechanistic insight from model systems. Angew Chem Int Ed 49:5628–5654
3. Wang SS, Liu KN, Chin J (2008) Membrane dipole potential of interaction between amyloid protein and phospholipid membranes is dependent on protein aggregation state. Inst Chem Eng 39:321–328
4. Friedman R, Pellarin R, Caflisch A (2009) Amyloid aggregation on lipid bilayers and its impact on membrane permeability. J Mol Biol 387:407–415
5. Nicolay JP, Gatz S, Liebig G, Gulbins E, Lang F (2007) Amyloid induced suicidal erythrocyte death. Cell Physiol Biochem 19(1–4):175–184
6. Misiti F, Orsini F, Clementi ME, Masala D, Tellone E, Galtieri A, Giardina B (2008) Amyloid peptide inhibits ATP release from human erythrocytes. Biochem Cell Biol 86(6):501–508
7. Clementi ME, Giardina B, Colucci D, Galtieri A, Misiti F (2007) Amyloid-beta peptide affects the oxygen dependence of erythrocyte metabolism: a role for caspase 3. Int J Biochem Cell Biol 39(4):727–735
8. Kosenko EA, Solomadin IN, Kaminsky YG (2009) Effect of the β-amyloid peptide Aβ25–35 and fullerene C60 on the activity of enzymes in erythrocytes. Russ J Bioorg Chem 35(2):157–162
9. van Rensburg SJ, Carstens ME, Potocnik FC, Aucamp AK, Taljaard JJ, Koch KR (1992) Membrane fluidity of platelets and erythrocytes in patients with Alzheimer's disease and the effect of small amounts of aluminium on platelets and erythrocytes membrane. Neurochem Res 17(8):825–829
10. Ajmani RS, Metter EJ, Jaykumar R, Ingram DK, Spangler EL, Abugo OO, Rifkind JM (2000) Hemodynamic changes during aging associated with cerebral blood flow and impaired cognitive function. Neurobiol Aging 21(2):257–269
11. Mattson MP, Begley JG, Mark RJ, Furukawa K (1997) Abeta 25–35 induces rapid lysis of red blood cells: contrast with Abeta1-42 and examination of underlying mechanisms. Brain Res 771(1):147–153
12. Perry RT, Gearhart DA, Wiener HW, Harrell LE, Barton JC, Kutlar A, Kutlar F, Ozcan O, Go RC, Hill WD (2008) Hemoglobin binding to Aβ and HBG2 SNP association suggest a role in Alzheimer's disease. Neurobiol Aging 29(2):185–193
13. Shaklai N, Yguerabide J, Ranney HM (1977) Interaction of hemoglobin with red blood cell membranes as shown by a fluorescent chromophore. Biochemistry 16(25):5585–5592
14. Shaklai N, Yguerabide J, Ranney HM (1977) Classification and localization of hemoglobin binding sites on the red blood cell membrane. Biochemistry 16(25):5593–5597
15. Eisinger J, Flores J, Salhany JM (1982) Association of cytosol hemoglobin with the membrane in intact erythrocytes. Proc Natl Acad Sci USA 79:408–412
16. Demehin AA, Abugo OO, Jayakumar R, Lakowicz JR, Rifkind JM (2002) Binding of hemoglobin to red cell membranes with eosin-5-maleimide-labeled band 3: analysis of centrifugation and fluorescence lifetime data. Biochemistry 41:8630–8637
17. Szundi I, Szelényi JG, Breuer JH, Bérczi A (1980) Interactions of haemoglobin with erythrocyte membrane phospholipids in monomolecular lipid layers. Biochim Biophys Acta 595(1):41–46
18. Papahadjopoulos D, Moscarello M, Eylar EH, Isac T (1975) Effects of proteins on thermotropic phase transitions of phospholipid membranes. Biochim Biophys Acta 401:317–335
19. Kimelberg HK (1976) Protein-liposome interactions and their relevance to the structure and function of cell membranes. Mol Cell Biochem 10(3):171–190
20. Szebeni J, Hauser H, Eskelson CD, Watson RR, Winterhalter KH (1988) Interaction of hemoglobin derivatives with liposomes. Membrane cholesterol protects against the changes of hemoglobin. Biochemistry 27:6425–6434
21. Szebeni J, Di Iorio EE, Winterhalter KH (1985) Encapsulation of hemoglobin in phospholipid liposomes: characterization and stability. Biochemistry 24:2827–2832
22. Grunwald EW, Richards MP (2006) Mechanisms of heme protein-mediated lipid oxidation using hemoglobin and myoglobin variants in raw and heated washed muscle. J Agric Food Chem 54:8271–8280
23. Fu X, Xu S, Wang Z (2009) Kinetics of lipid oxidation and off-odor formation in silver carp mince: the effect of lipoxygenase and hemoglobin. Food Res Int 42:85–90
24. Ioffe VM, Gorbenko GP, Deligeorgiev T, Gadjev N, Vasilev A (2007) Fluorescence study of protein-lipid complexes with a new symmetric squarylium probe. Biophys Chem 128:75–86
25. Mui B, Chow L, Hope MJ (2003) Extrusion technique to generate liposomes of defined size. Meth Enzymol 367:3–14
26. Bartlett G (1959) Phosphorus assay in column chromatography. J Biol Chem 234(3):466–468
27. Holley M, Eginton C, Schaefer D, Brown LR (2008) Characterization of amyloido-genesis of hen egg lysozyme in concentrated ethanol solution. Biochem Biophys Res Commun 373:164–168
28. Krasnowska EK, Gratton E, Parasassi T (1998) Prodan as a membrane surface fluorescence probe: partitioning between water and phospholipid phases. Biophys J 74:1984–1993
29. Lakowicz JR (2006) Principles of fluorescent spectroscopy, 3rd edn. Springer, Singapore
30. Li SJ, Nakagawa A, Tsukihara T (2004) Ni^{2+} binds to active site of hen egg-white lysozyme and quenches fluorescence of Trp62 and Trp108. Biochem Biophys Res Commun 324:529–533
31. Formoso C, Forster LS (1975) Tryptophan fluorescence lifetimes in lysozyme. J Biol Chem 250:3738–3745
32. Booth DR, Sunde M, Bellotti V, Robinson CV, Hutchinson WL, Fraser PE, Hawkins PN, Dobson CM, Radford SE, Blake CC, Pepys MB (1997) Instability, unfolding and aggregation of human lysozyme variants underlying amyloid fibrillogenesis. Nature 385:787–793
33. Conio G, Patrone E, Brighetti S (1970) The effect of aliphatic alcohols on the helix-coil transition of poly-L-ornithine and poly-L-glutamic acid. J Biol Chem 245:3335–3340
34. Tanaka S, Oda Y, Ataka M, Onuma K, Fujiwara S, Yonezawa Y (2001) Denaturation and aggregation of hen egg lysozyme in aqueous ethanol solution studied by dynamic light scattering. Biopolymers 59:370–379
35. Manning LR, Jenkins WT, Hess JR, Vandegriff K, Winslow RM, Manning JM (1996) Subunit dissociations in natural and recombinant hemoglobins. Protein Sci 5:775–781
36. Kremer JJ, Pallito MM, Sklansky DJ, Murphy RM (2000) Correlation of β-amyloid aggregate size and hydrophobicity with decreased bilayer fluidity of model membranes. Biochemistry 39:10309–10318
37. Bolton W, Perutz MF (1970) Three dimensional Fourier synthesis of horse deoxyhaemoglobin at 2.8 Å resolution. Nature 228:551–552
38. Bossi L, Alema S, Calissano P, Marra E (1975) Interaction of different forms of haemoglobin with artificial lipid membranes. Biochim Biophys Acta 375:477–482
39. Beppu M, Nagoya M, Kikugawa K (1986) Role of heme compounds in the erythrocyte membrane damage induced by lipid hydroperoxide. Chem Pharm Bull 34(12):5063–5070
40. Carvajal AK, Rustad T, Mozurait yte R, Storro I (2009) Kinetic studies of lipid oxidation induced by hemoglobin measured by consumption of dissolved oxygen in a liposome model system. J Agric Food Chem 57:7826–7833
41. Trusova VM, Gorbenko GP, Deligeorgiev T, Gadjev N, Vasilev A (2009) A novel squarylium dye for monitoring oxidative processes in lipid membranes. J Fluoresc 19:1017–1023
42. Hoff B, Strandberg E, Ulrich AS, Tieleman DP, Posten C (2005) ^{2}H-NMR study and molecular dynamics simulation of the location, alignment, and mobility of pyrene in POPC bilayers. Biophys J 88:1818–1827
43. Duportail G, Lianos P (1996) Fluorescence probing of vesicles using pyrene and pyrene derivatives. In: Rosoff M (ed) Vesicles. Marcel Dekker, Inc, New York, pp 295–371

44. Kaprovich DS, Blanchard GJ (1995) Relating the polarity-dependent fluorescence response of pyrene to vibronic coupling. Achieving a fundamental understanding of the py polarity scale. J Phys Chem 99:3951–3958
45. Xi J, Guo R, Guo X (2006) Interactions of hemoglobin with lecithin liposomes. Colloid Polym Sci 284:1139–1145
46. Klymchenko AS, Duportail G, Demchenko AP, Mely Y (2004) Bimodal distribution and fluorescence response of environment-sensitive probes in lipid bilayers. Biophys J 86:2929–2941
47. Gornicki A (2003) The influence of oxidative stress on microviscosity of hemoglobin-containing liposomes. Gen Physiol Biophys 22:121–127
48. Barenholz Y, Cohen T, Haas E, Ottolenghi M (1996) Lateral organization of pyrene-labeled lipids in bilayers as determined from the deviation from equilibrium between pyrene monomers and excimers. J Biol Chem 271(6):3085–3090
49. Blackwell MF, Gounaris K, Barber J (1986) Evidence that pyrene excimer formation in membranes is not diffusion-controlled. Biochim Biophys Acta 858:221–234